

A Thermodynamic Model for Asphaltene and Wax Precipitation Simultaneously using Multi-Solid Method

Z. Nasri^{a,b}; B. Dabir^{a,c*}

ABSTRACT

A thermodynamic model based on multi-solid theory to predict asphaltene and wax precipitation has been developed. The pseudo-components of crude oil are estimated as paraffinic, naphthenic and aromatic portions. The model is capable of predicting the amount of asphaltene precipitation caused by pressure changes and solvent injection. The predictions of the proposed model are compared to experimental data adopted from available literature and those of the other models. The results of the present model are satisfactory. The effects of temperature, molecular weight of solvent, resin, carbon number, addition of an aromatic and wax and asphaltene precipitation simultaneously are also represented. The effect of temperature on wax precipitation is also performed and the predictions are compared to experimental data.

KEYWORDS

Asphaltene precipitation; Multi-solid Method; Wax precipitation.

1. INTRODUCTION

Paraffins, asphaltenes and resins are the typical sources of organic deposition in wells, pipelines, and reservoir formation during petroleum production[1]. Asphaltenes are defined as "the wax-free fraction of crude oil that is insoluble in n-heptane but soluble in hot toluene/benzene" (ASTM 6560). Resins are defined as the fraction of crude oil that is insoluble in propane but soluble in n-heptane.

Asphaltenes have high density polyaromatic structures with polydispersity property containing different atoms and metals existing in crude oils and are surrounded and stabilized by resins. Pentane and heptane are the two solvents which are used to separate asphaltenes from crude oil. Resins are also polar and aromatic molecules containing different atoms and metals that surround asphaltenes and help keep them in suspension.

Asphaltene induced damage can be explained by three mechanisms [2].

1-The increase of the reservoir fluid viscosity by formation of a water-in-oil emulsion.

2- The change of the wettability of the reservoir formation from water-wet to oil-wet by the adsorption of asphaltenes over the pore surface in the reservoir formation.

3-The impairment of the reservoir formation permeability by plugging of the pore throats by asphaltene particles.

The precipitation mechanism of wax and asphaltenes are significantly different. Asphaltene aggregates; wax crystallizes or solidifies and precipitates due to high saturation. The stability of asphaltenes is affected by the environment; the wax stability depends on temperature and composition. Paraffinic waxes are non-polar molecules, whereas asphaltenes are polar ones containing hydrogen bonds. These differences cause different changes in waxes and asphaltene phase behaviour.

Wax and asphaltene precipitation are different processes; the effects of composition, pressure and temperature on wax precipitation can be in the opposite direction to those on asphaltene precipitation. An increase in pressure enhances wax precipitation, but can inhibit asphaltene precipitation. Wax precipitation is strongly affected by temperature; temperature may weakly affect asphaltene precipitation, and may enhance or inhibit it. The composition effect is also very different on wax and asphaltene precipitation. An increase in concentration of light hydrocarbons such as C3 and C5 and non-hydrocarbons such as CO2 decrease wax precipitation. On the other hand, an increase in the amount of these species can significantly enhance asphaltene precipitation. The mixing of a crude oil with some polar species in small

a. Chemical Engineering Department, Amirkabir University of Technology, Tehran, Iran (email: drbdabir@aut.ac.ir).

b. Institute of Chemical Technologies, Iranian Research Organization for Science and Technology, Tehran, Iran.

c. Energy Research Center, Amirkabir University of Technology, Tehran, Iran.

amounts may have a strong effect on asphaltene precipitation [3].

A comparison between the specifications of wax and asphaltene precipitation is represented in Table 1.

In the present model, a thermodynamic model to predict the amounts of asphaltene and wax precipitation is developed.

TABLE 1
COMPARISON BETWEEN THE SPECIFICATIONS OF
WAX AND ASPHALTENE PRECIPITATION

	Asphaltenes	Waxes
Precipitation Causes	High pH , Injecting Low Surface Tension Fluids (light paraffins , Pentane , Hexane , ... , Gas Condensates) Pressure	Cooling High Pressure Drop
Precipitation Region	Large distance from the wellbore	Short distance from the wellbore (0 to 1 feet)
Precipitation Mechanism	Aggregation	Crystallization
Temperature Effect	Weak Effect (high temperature)	Strong Effect (low temperature)
Pressure Effect	Strong Effect	Weak Effect
Thermodynamic Model	Reversible and irreversible	Reversible
Polar	+	-

2. REVIEW OF WAX AND ASPHALTENE PRECIPITATION THERMODYNAMIC MODELS

References [4] and [5] proposed a model to study wax precipitation in two and three phases which is based upon Regular Solution Theory and used Soave-Redlich-Kwong (SRK) Equation of State to predict phase behavior. References [6] and [7] have shown that wax precipitated from a petroleum fluid consists of normal paraffins, iso-paraffins, and naphthenes. Aromatics are not precipitated as wax. Reference [8] based upon the observations of [9] developed a thermodynamic multisolid wax model. Reference [10] represented a thermodynamic model to describe wax precipitation based on Flory-Free-Volume model for the liquid phase and a predictive form of Wilson equation for the nonideality of the solid solution. References [11] and [12] studied wax precipitation for gas condensate fluids.

Asphaltene precipitation is modeled using a variety of methods. In general, there are two points of view with regard to asphaltene precipitation; some models have

considered this process, like the other components, as reversible process and allow the use of phase equilibria calculations. On the other hand, the other models have assumed that the process of asphaltene precipitation is irreversible since asphaltene particles are suspended and stabilized by resins. According to these models, when resins are removed, asphaltenes precipitate irreversibly. The recent models have emphasized on the reversibility of asphaltene precipitation.

A. Solubility Models

These models have been developed based upon Flory-Huggins theory and admit that asphaltene precipitation is a reversible process. In all these models, at first, a liquid-vapor equilibrium is performed to determine the liquid phase properties. Then a pseudo-liquid-liquid equilibrium calculation is conducted and it is assumed that the asphaltene precipitation will not affect the liquid-vapor equilibrium. These models are divided into monodisperse and polydisperse models. In the first group, the complex mixture of asphaltenes is characterized by one pseudo-component with average properties to identify the whole family. In the second group, the asphaltene compound is characterized by using a distribution function with one or two variables. Molecular weight of asphaltenes usually is used as a variable.

Reference [13] used for the first time the Flory-Huggins theory to predict the onset of asphaltene. The model admits that the crude oil is a homogeneous mixture of asphaltene and solvent. References [14], [15] and [16] developed a model based on statistical thermodynamic of polymer solutions. Hirschberg's model is modified by considering that asphaltenes precipitate as a non-pure phase [17].

References [18] and [19] employed for the first time a distribution function to characterize the asphaltenes. Then Scott-Magat polymer solution theory is used with gamma function as the distribution function [18]. Reference [19] used another analytical function based upon the fractal aggregation theory, as proposed in [20]. Reference [19] obtained satisfactory results for asphaltene precipitation of a stock tank oil but the model proposed poor results at high pressures.

Reference [21] also employed a distribution function to characterize asphaltenes. They obtained several subcomponents experimentally. This model is used for polar and non-polar solvents. Reference [22] employed a bivariate distribution function to characterize the composition of asphaltenes. The molecular weight of asphaltenes and H/C ratio of the components are the variables. Reference [23] represented a model based upon polydisperse solution mechanism associated with aggregation kinetic theory.

Reference [24] developed a thermodynamic model to

predict asphaltene precipitation in crude oil under reservoir conditions. In this model, asphaltenes are characterized as a continuous family that follows a distribution function based upon the fractal aggregation theory. Discretization of the function is made by using roots of an orthogonal polynomial. A satisfactory representation of the experimental data is obtained.

B. Solid Models

These models have considered asphaltene as one component in solid phase and use the cubic EOS to model liquid and vapor phases. Reference [25] has presented a model to predict asphaltene precipitation by taking into account asphaltenes as a solid phase. Asphaltenes have been divided into two pseudo-components, one precipitating and the other non-precipitating. The precipitating one is considered asphaltene. The amount of asphaltene precipitated is obtained by making equivalent the fugacity of asphaltene component in liquid and solid phases. Additionally, a three-phase calculation is conducted.

C. Association Models

Association theory is an important subject in thermodynamics. The most common application of this model is related to fluids containing hydrogen bonds which molecules attach to each other to form dimers and trimers. Reference [26] proposed an association model incorporated in the Peng Robinson Equation of State (PR EOS) for predicting water/reservoir crudes phase behavior. Reference [27] represented a method for application of EOS for associating fluids using the analytic chain association theory (ACAT). The model is used to calculate density and vapor pressure of water, ammonia, and methanol as the three representative associating fluids. Reference [28] developed an association model using PR-EOS to predict asphaltene precipitation and to explain the liquid-vapor phase behavior. In that model the association term is incorporated in the EOS.

D. Colloid Model

This model assumes asphaltene precipitation process is irreversible. Reference [29] proposed a colloidal model which is developed in [14] and [15]. According to this model, the asphaltene particles are stabilized and suspended by resin molecules. Critical point is a situation where the resin concentration is such that a monolayer of resins remains around the asphaltene particles. After this point when the resin concentration reduces, asphaltene precipitates. Reference [30] has stated that this model results are satisfactory in determining the onset of asphaltene precipitation, but are not good for the quantity of deposited asphaltene. Reference [17] also has reported this result.

E. Micellization Model

Reference [31] proposed a micellization model for asphaltene precipitation. It is assumed that asphaltene molecules form a micellar core and the resin molecules surrounded and are adsorbed on asphaltene core. The minimization of Gibbs free energy is used to determine micelle structure and concentration. A satisfactory representation of micellar size was obtained, but the results do not include the quantity of asphaltene precipitated.

F. Fractal Aggregation Models

According to statistical physics, there are three principal models of fractal aggregation:

- 1-Diffusion Limited Aggregation (DLA)
- 2-Diffusion Limited Cluster-Cluster Aggregation (DLCC)
- 3-Reaction Limited Cluster-Cluster Aggregation (RLCC)

The experimental observations by X-ray scattering methods and the microscopic observations of solution including asphaltenes precipitated show that asphaltene aggregation follows these models. In the first model, aggregation mechanism will occur by attaching the particles and is controlled by diffusion. In the second model, aggregation will occur by attaching the small aggregated particles to the large ones. In the third model, it is assumed that aggregation is controlled by reaction between the aggregates. References [32], [33], [34], and [35] showed that the titration curves of a crude oil including asphaltene can produce a universal equation which is similar to the universal equations in association process.

3. A MULTI-SOLID MODEL TO PREDICT WAX AND ASPHALTENE PRECIPITATION SIMULTANEOUSLY (PRESENT MODEL)

In this paper, a multi-solid model to calculate the quantity of wax and asphaltene precipitation is developed. Studies show that when a binary normal alkane mixture is cooled, the precipitation is unstable and segregates into two solid phases, providing the chain-length difference between the two alkanes exceeds a certain value [3].

At first, a thermodynamic multi-solid wax model is developed [6]. In this model, each solid phase is described as a pure component which does not mix with the other solid phases. According to the stability analysis, a component may exist as a pure solid if

$$f_i(P, T, Z) - f_{pure,i}^S(P, T) \geq 0 \quad i=1, \dots, c \quad (1)$$

where $f_i(P, T, Z)$ is the fugacity of component i with feed composition z . The components that fulfill (1) will precipitate.

In the present model, in order to calculate the physical properties of components, the pseudo-components are subdivided into paraffinic, naphthenic and aromatic (PNA) groups.

There is the following expression between the fugacity of a pure solid component i (f_{Si}^o) and the fugacity of that component in liquid phase (f_{li}^o), with considering various solid-state transitions [12]:

$$\ln \left[\frac{f_{li}^o}{f_{Si}^o} \right] = \frac{\Delta H_i^f}{RT} \left[1 - \frac{T}{T_i^f} \right] + \sum_{j=1}^n \frac{\Delta H_{ij}^{lr}}{RT} \left[1 - \frac{T}{T_{ij}^{lr}} \right] + \frac{\Delta C_{pi}}{R} \left[1 - \frac{T_i^f}{T} - \ln \left[\frac{T}{T_i^f} \right] \right] + \sum_{j=1}^n \frac{\Delta C_{pj}}{R} \left[1 - \frac{T}{T_{ij}^{lr}} - \ln \left[\frac{T}{T_{ij}^{lr}} \right] \right] \quad (2)$$

where ΔH_i^f and T_i^f are enthalpy of fusion and melting-point temperature, respectively. ΔC_{pi} is the heat capacity of fusion. ΔH_{ij}^{lr} is the enthalpy of the j -solid transition and T_{ij}^{lr} is the j -solid-state transition temperature.

By neglecting the effect of the heat capacities of solid-state transitions and with applying simplifications on the second term on the right hand side of (1), the following expression may be obtained:

$$\ln \left[\frac{f_{li}^o}{f_{Si}^o} \right] = \frac{\Delta H_i^f}{RT} \left[1 - \frac{T}{T_i^f} \right] + \frac{\sum_{j=1}^n \Delta H_{ij}^{lr}}{RT} \left[1 - \frac{T}{T_{ij}^{lr}} \right] + \frac{\Delta C_{pi}}{R} \left[1 - \frac{T_i^f}{T} - \ln \left[\frac{T}{T_i^f} \right] \right] \quad (3)$$

At specified temperature and pressure, for each component i , the equilibrium between liquid, vapor and multi-solid phases are expressed by the following equations.

Precipitating components:

$$f_i^v = f_i^l = f_{pure, i}^s \quad (4)$$

Non-precipitating components:

$$f_i^v = f_i^l \quad (5)$$

In order to calculate the fugacity of a pure solid component i ($f_{pure, i}^s$), it is required to obtain the melting-point temperature (T_i^f), the enthalpy of fusion (ΔH_i^f), the heat capacity of fusion (ΔC_{pi}), the transition temperature and enthalpy (T_{ij}^{lr} , ΔH_{ij}^{lr}), the critical points and acentric factor of component i . These properties for pure components and pseudo-components which are subdivided into PNA groups are calculated by using the correlations obtained from the literature. For asphaltenes and resin components, the properties such as T_i^f , ΔH_i^f and PR-EOS parameters (a , b) are adjusted to fit experimental data available from the literature. The Nelder-Mead method or Simplex method which is a commonly used nonlinear optimization algorithm is applied to minimize the sum of relative errors as an objective function [36].

A. Binary Interaction Coefficients

The binary interaction coefficients between methane and the other n-alkanes are estimated by the following correlations [37].

$$K_{ij} = 0.0289 + 1.633 \times 10^{-4} MW_j \quad (6)$$

for two n-alkanes:

when ($MW_i < 255, MW_i < MW_j$)

$$K_{ij} = f_1 + f_2 \ln(MW_i) + f_3 \frac{\ln(MW_i)}{MW_i^2} \quad (7)$$

in which

$$f_1 = 0.2578761 + 0.0001 MW_j$$

$$f_2 = 0.05498 - 3.864 \times 10^{-5} MW_j$$

$$f_3 = 55.3282 - 0.04085 MW_j$$

when ($MW_i \geq 255, MW_i \leq MW_j$)

$$K_{ij} = 0 \quad (8)$$

The binary interaction coefficients between n-alkanes and non n-alkanes and also between two non n-alkanes due to minor effects on results are considered to be zero.

B. Characterization Method

A semi continuous method represented in [38] is used to characterize the heavy-end component of a crude oil.

In this model, a Gaussian-laguerre quadrature function has been used. The upper limit of carbon number and the number of pseudo-components are as input parameters and the carbon number and the mole fraction of each pseudo-component are as output parameters. The upper limit of carbon number may be 50 or more. The carbon number more than 70 is not common in crude oil. The number of pseudo-components usually is selected between 3 and 6.

C. Discretization of Pseudo-Components to PNA Groups

According to [39] the paraffinic, naphthenic, and aromatic portions of pseudo-components can be predicted from two sets of properties:

- 1- Specific gravity, refractive index, and viscosity.
- 2- Molecular weight, refractive index, and carbon to hydrogen weight ratio.

The proposed correlations may be used for fractions with molecular weights of 70-600.

In the present model, the second method is applied. Molecular weight (M), refractive index (n) and carbon to hydrogen ratio (C/H) are calculated from the correlations represented in the literature [40], [41], [39], [42], [43].

D. Fugacity of A Pure Solid Component

The fugacity of a pure solid component is estimated from (2), in which the following properties are required.

1) Melting-Point Temperature

The melting-point temperature of n-alkanes is estimated from the correlation proposed in [4] and those of aromatics, naphthenes and paraffins are calculated from the correlation represented in [6].

2) Enthalpy of Fusion

For the enthalpies of fusion the following correlations are used.

The correlation proposed in [4] for paraffins and the correlation given in [44] for aromatics and the correlation proposed in [6] for aromatics, naphthenes and isoparaffins.

3) Transition Temperature and Enthalpy

Fusion properties of n-alkanes with odd and even carbon numbers are different. This difference is essentially caused by steric effects from the rearrangement of atoms in the molecules [12].

In the present model, the correlations proposed in [45] are used to estimate transition temperature and enthalpy of components.

4) Heat Capacity of Fusion

The correlation represented in [46] is admitted to calculate heat capacity of fusion for alkanes, naphthenes and aromatics.

5) Critical Properties of Light Components and Pseudo-Components

These properties are estimated using the correlations proposed in [47] and [48]. The correlation of [48] is analyzed for hydrocarbon components including paraffins, olefins, naphthenes and aromatics; the results are satisfactory. In this method, a group of n-alkanes is used as a reference system to predict the properties of the other hydrocarbons.

Critical temperature, critical volume, specific gravity and molecular weight of n-alkanes from C_1 to C_{100} are obtained in terms of a function of normal boiling point accurately. At each specific boiling point, one n-alkane is determined that has the same boiling point by trial and error and using this n-alkane the properties of the pseudo-component are calculated with applying the properties of reference system.

The critical properties of PNA groups are estimated using the correlations represented in [47]. The correlation developed in [45] is admitted to calculate acentric factor of heavy aromatics. For aromatic components with molecular weight more than 800, $w=2$ has been taken into account. The method presented in [47] is used to calculate the acentric factor of paraffin and naphtene components.

4. APPLICATIONS OF THE PRESENT MODEL

Two different sets of experimental data are applied to evaluate the present model for asphaltene precipitation.

A. Effect of Pressure

Table 2 reports the composition of oil (1) [49] used to evaluate the effect of pressure on asphaltene precipitation. In order to characterize the heavy-end component, the method developed by Behrens and S. I. Sandler is used [38]. Table 3 shows the characterization of oil (1) using this method. The C_7+ component is subdivided into 9 pseudo-components; the last four ones are asphaltenes.

TABLE 2

COMPONENTS AND COMPOSITIONS OF OIL (1)

Component	Composition (mol%)
Nitrogen	0.57
CO ₂	2.46
Methane	36.37
Ethane	3.47
Propane	4.05
i-Butane	0.59
n-Butane	1.34
i-Pentane	0.74
n-Pentane	0.83
Hexanes	1.62
Heptane plus	47.96
Total	100
C ₇₊ molecular weight	329
C ₇₊ specific gravity	0.9594
Live-oil molecular weight	171.4
Asphaltene content in stock-tank oil, wt%	16.8
Reservoir temperature, oC	100
Saturation Pressure, atm	200.68

Fig. 1 shows a comparison between the results of the model and experimental data. The calculated points from the other models obtained from the literature are also shown in this figure. As it can be seen, according to the experimental data, the pressure in which the maximum precipitation is occurred is 137 atm. However, the present model predicts the maximum precipitation is occurred at 206 atm (out of the four available points). As the saturation pressure of oil (1) is 201 atm [49] and the maximum precipitation is taken place at the saturation pressure, the prediction of the present model is correct and shows the weak point of the experimental data. However, the results of the other model [31] are far from experimental data, could shows this weak point.

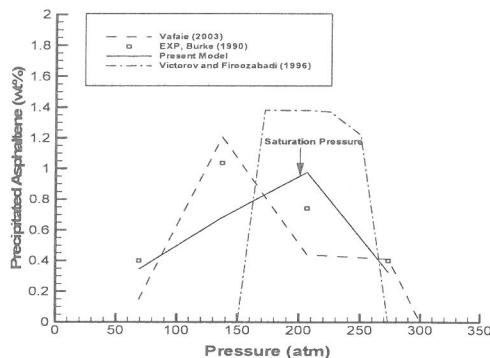


Figure 1: A comparison between the results of the present model and experimental data for oil (1).

B. Effect of Solvent Injection

Table 4 shows the composition of oil (2) used to assess the effect of solvent addition [50]. Table 5 shows the characterization of oil (2) by using the method proposed in [38]. The C_7+ component is subdivided into 9 pseudo-components; the three last ones are asphaltenes.

Fig. 2 compares the predicted values using the present model and experimental data. The result of the other model [51] is shown in this figure. The cause of precipitation is CO_2 injection and with increasing solvent, the amount of precipitation is increased.

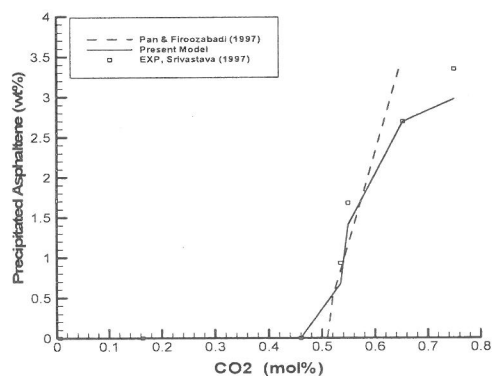


Figure 2: A comparison between the results of the present model and experimental data for oil (2).

C. Effect of Temperature

Fig. 3 shows the effect of pressure on asphaltene precipitation at different temperatures for oil (1). It should be considered that these predictions are performed using the adjusted parameters obtained in the part of effect of pressure. Therefore, these results show the application of the model qualitatively. Fig. 4 depicts the precipitation with changes in temperature at different pressures. All profiles have a maximum point and the precipitation is increased as pressure increases.

It is evident that this is correct just at the studied range of pressure and over saturation pressure the precipitation will decrease. These results are in agreement with the results of the previous investigators [23], [52], [16] and are obtained from experimental analysis as well [52], [53]. According to this figure at above saturation pressure, the asphaltene solubility has been changed abruptly which is in accordance with the conclusions of the some other researchers [23][53].

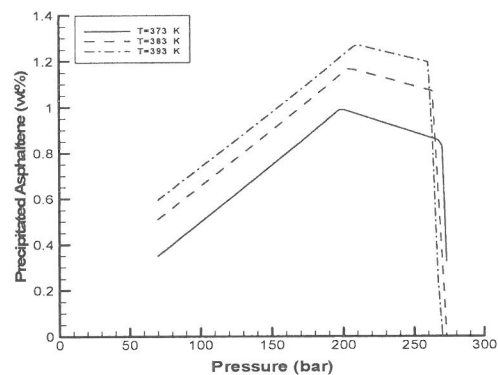


Figure 3: Effect of pressure on asphaltene precipitation at different temperatures for oil (1).

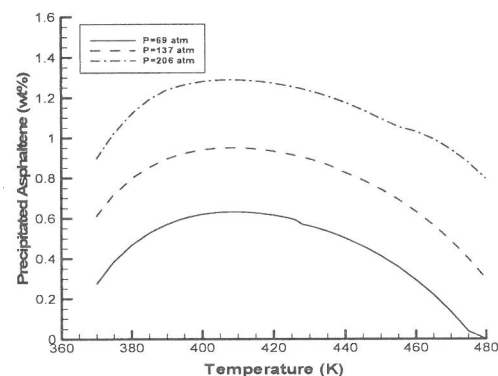


Figure 4: Effect of temperature on asphaltene precipitation at different pressure for oil (1).

D. Effect of Solvent Molecular Weight

Fig. 5 shows the effect of n-alkanes molecular weight as solvent on asphaltene precipitation in different amounts of solvent injection for oil (1). Evidently, the precipitation is decreased with increasing solvent molecular weight. The increasing of solvent molecular weight results in increasing of crude oil molecular weight.

The heavier crude oil solves more asphaltene. This result is in accordance with the works of the other researchers [52], [1]. It can be seen from Fig. 5, for lighter solvents (left side of the figure), the precipitation increases with increasing mole fraction of the solvent and vice versa for heavier solvents (right side of the figure). The results are in concordance with expected physical behavior.

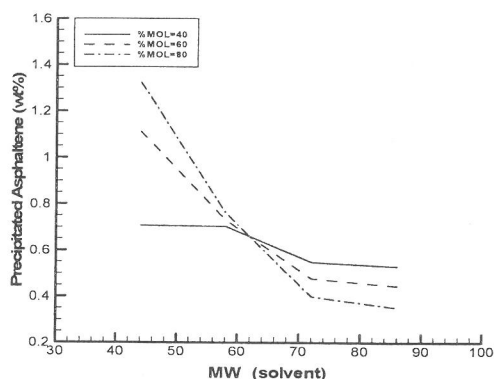


Figure 5: Effect of n-alkanes molecular weight as solvent on asphaltene precipitation for oil (1).

E. Effect of Resin

Fig. 6 shows the effect of resin on asphaltene precipitation for oil (1) in two different amounts of resin. Obviously, as resin increases, the asphaltene precipitation declines. This result is according to the theory of asphaltene precipitation in which the asphaltene particles are stabilized and suspended by resins and when resin concentration reduces, asphaltene flocculation occurs.

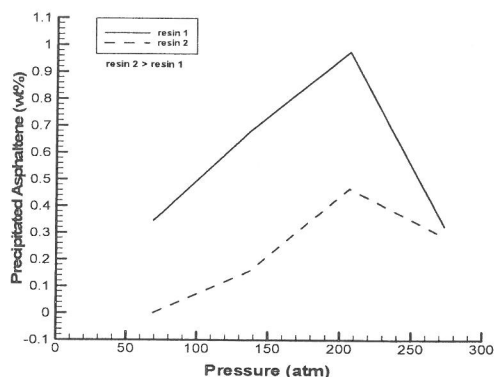


Figure 6: Effect of resin injection on asphaltene precipitation for oil (1).

G. Effect of Aromatics

Fig. 7 shows the effect of increasing an aromatic (Benzene) on asphaltene precipitation at two different pressures. This result is obtained by change of the aromatic composition in oil (1). The increasing of benzene causes decreasing of precipitation. Furthermore, the quantity of precipitation is increased with increasing pressure (in the studied range).

Considering that aromatics such as benzene and toluene are solvent of asphaltene, this result is reasonable.

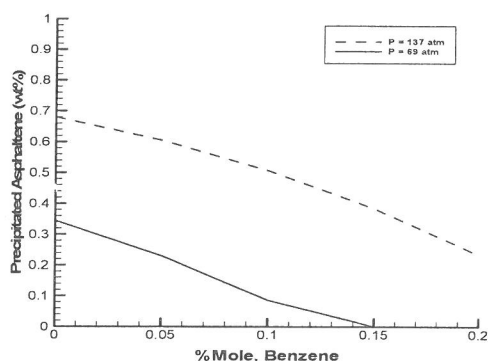


Figure 7: Effect of an aromatic injection on asphaltene precipitation for oil (1).

H. Wax Precipitation

The composition of oil presented in [12] and [44] is used to predict wax precipitation. Due to lacking of asphaltene in the oil, the parameters of the model are not adjusted to fit experimental data. Fig. 8 shows the comparison of the model results with experimental data [37].

I. Precipitation of Wax and Asphaltene Simultaneously

Fig. 9 shows the precipitation of wax and asphaltene simultaneously for oil (1). As it can be seen, at high temperatures only asphaltene precipitates and wax precipitates in low temperatures.

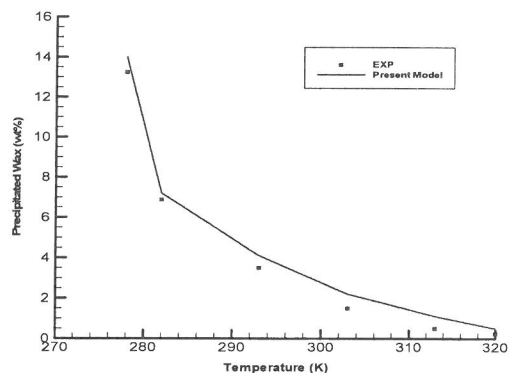


Figure 8: A comparison between results of the model and experimental data for oil (3). (Wax precipitation)

5. DISCUSSION AND RESULTS

A thermodynamic model is developed with the following specifications:

- 1- The model is based on a multi-solid phase.
- 2- The C7+ component of crude oil after characterization is subdivided to PNA groups.
- 3- The model can predict the wax and asphaltene precipitation in the reservoir conditions.
- 4- Effect of pressure and increasing solvent on asphaltene precipitation is predicted and the results are compared with experimental data and the results of some other

models adopted from the literature, showing a better agreement than the earlier models.

5- The prediction of the model regarding the effect of temperature on wax precipitation is compared to experimental data.

6- The effects of temperature, molecular weight of solvent, resin, carbon number of solvent and injection an aromatic on asphaltene precipitation are predicted by the present model. The results are in agreement with the earlier models.

7- In the case of asphaltene precipitation, the model can determine an error in the experimental data of a famous crude oil.

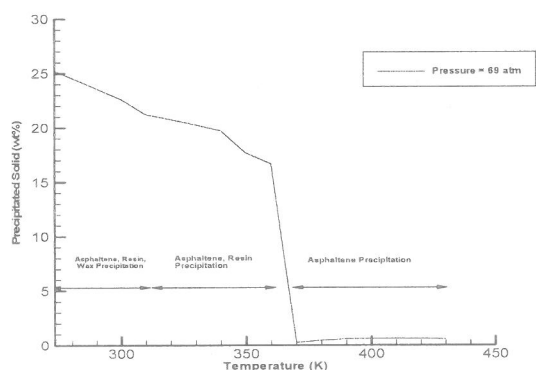


Figure 9: the precipitation of wax and asphaltene simultaneously for oil (1).

6. NOMENCLATURE

a	PR-EOS parameter
b	PR-EOS parameter
AS	asphaltene
C/H	carbon to hydrocarbon weight ratio
f_i	fugacity of component i in feed, bar, atm
f_i^l	fugacity of component i in liquid phase, bar, atm
f_i^v	fugacity of component i in vapor phase, bar, atm
f_i^o	fugacity of component i in liquid phase, bar, atm
$f_{pure,i}^s$	fugacity of component i in solid phase, bar, atm
f_{si}^o	fugacity of component i in solid phase, bar, atm
K_{ij}	binary interaction coefficient
MW	molecular weight of component, g/mol
n	number of component in feed
P	pressure, bar, atm
PNA	paraffinic, naphtenic and aromatic groups
PR	Peng Robinson EOS
PS	pseudo-component
R	gas constant
RS	resin
T	temperature, C, K
T_i^f	fusion temperature of component i, K
T_{ij}^{tr}	j solid-state transition temperature of component i, K
w	acentric factor
Z	mole fraction of component i in feed

Greek Letters

ΔC_{pi}	heat capacity of fusion, cal/K-mol
ΔH_i^f	enthalpy of fusion, cal/mol
ΔH_{ij}^{tr}	enthalpy of the J-solid transition of component i, cal/mol

subscripts

i	indice of components
j	indice of components

7. APPENDIX

TABLE 3: CHARACTERIZATION OF OIL (1)

Component	%mol	MW(g/mol)
Nitrogen	0.57	28.12
CO2	2.46	44.01
Methane	36.37	16.04
Ethane	3.47	30.54
Propane	4.05	44.1
i-Butane	0.59	58.12
n-Butane	1.34	58.12
i-Pentane	0.74	72.15
n-Pentane	0.83	72.15
Hexanes	1.62	86.18
PS-1	7.53	103.08
PS-2	13.1	171.44
PS-3	12.2	291.08
PS-4	8.09	455.64
RS	4.18	654.56
AS-1	1.81	871.67
AS-2	0.706	1083.99
AS-3	0.259	1262.22
AS-4	0.0778	1375.15

TABLE 4: COMPONENTS AND COMPOSITIONS OF OIL (2)

Component	%mol
Nitrogen	0.96
CO2	0.58
H2S	0.3
Methane	4.49
Ethane	2.99
Propane	4.75
i-Butane	0.81
n-Butane	1.92
i-Pentane	1.27
n-Pentane	2.19
C6-C9	25.73
C10-C17	26.98
C18-C27	13.28
C28+	13.75
Total	100
molecular weight	230
Asphaltene content, wt%	4.8
Reservoir temperature, oC	59
Saturation Pressure, Mpa	2.89

TABLE 5: CHARACTERIZATION OF OIL (2)

Component	%mol	MW
Nitrogen	0.96	28.12
CO ₂	0.58	44.01
H ₂ S	0.3	34.076
Methane	4.49	16.04
Ethane	2.99	30.54
Propane	4.75	44.1
i-Butane	0.81	58.12
n-Butane	1.92	58.12
i-Pentane	1.27	72.15
n-Pentane	2.19	72.15
PS-1	25.73	105
PS-2	26.98	179
PS-3	13.28	312
PS-4	7.034016	527.84
PS-5	3.708	855.47
RS	2.1782	1139.72
AS-1	0.500317	1338.08
AS-2	0.296479	1359.43
AS-3	0.032705	1402.29

9. REFERENCES

- [1] F. Civan, *Reservoir formation Damage: Fundamentals, Modeling, Assessment and Mitigation*, Gulf Publishing Company, Houston, Texas, 2000.
- [2] K. J. Leontaritis, "Asphaltene near-wellbore formation damage modeling," SPE 39446, SPE Formation Damage Control Conference, Lafayette, Louisiana, 1998.
- [3] A. Firoozabadi, *Thermodynamic of Hydrocarbon Reservoir*, Mc Graw-Hill, USA, 1999.
- [4] K. W. Won, "Thermodynamics for solid solution-liquid-vapor equilibria: Wax phase formation from heavy hydrocarbon mixtures," *Fluid Phase Equilibria*, vol. 30, pp. 265, 1986.
- [5] K. W. Won, "Thermodynamic calculation of cloud point temperatures and wax phase compositions of refined hydrocarbon mixtures," *Fluid Phase Equilibria*, vol. 53, pp. 377-396, 1989.
- [6] K. S. Pedersen, A. Fredenslund, and P. Thomassen, *Properties of Oils and Natural gases*, Gulf publishing Co., Houston, TX, 1989.
- [7] H. P. Ronningsen, B. Bjorndal, A. B. Hansen, and W. B. Pedersen, "Wax precipitation from North Sea crude oils. 1. Crystallization and dissolution temperatures, and Newtonian and non-newtonian flow properties," *Energy & Fuels*, vol. 5, pp. 895, 1991.
- [8] C. Lira-Galeana, A. Firoozabadi, and J. M. Prausnitz, "Thermodynamics of wax prediction in petroleum mixtures," *AIChE Journal*, vol. 42, pp. 239-248, 1996.
- [9] W. B. Pedersen, A. B. Hansen, E. Larsen, A. B. Nielsen, and H. P. Ronningsen, "Wax precipitation from North Sea crude oils. 2. Solid-phase content as function of temperature determined by pulsed NMR" *Energy & Fuels*, vol. 5, pp. 908, 1991.
- [10] J. A. P. Coutinho and V. Ruffier-Méray, "Experimental measurements and thermodynamic modeling of paraffinic wax formation in undercooled solutions," *Industrial & Engineering Chemistry Research*, vol. 36, pp. 4977-4983, 1997.
- [11] P. Ungerer, B. Faissat, C. Leibovici, H. Zhou, E. Béhar, G. Moracchini, and J. P. Courcy, "High pressure - high temperature reservoir fluids: Investigation of synthetic condensate gases containing a solid hydrocarbon," *Fluid Phase Equilibria*, vol. 111, pp. 287-311, 1995.
- [12] D. V. Nichita, L. Goual, and A. Firoozabadi, "Wax precipitation in gas condensate mixtures," *SPE Production & Facilities*, vol. 16, pp. 250-259, 2001.
- [13] A. Hirschberg, L. N. J. Dejong, B. A. Schipper, and J. G. Meijer, "Influence of temperature and pressure on asphaltene flocculation," *Society of Petroleum Engineers Journal*, vol. 24, pp. 283-293, 1984.
- [14] S. J. Park, G. A. Mansoori, "Aggregation and deposition of heavy organics in petroleum crude," *Energy Sources*, vol. 10, pp. 109-125, 1988.
- [15] S. J. Park and G. A. Mansoori, "Organic deposition from heavy petroleum crude," presented at the 4th International Conference on Heavy Crudes and Tar Sands, Edmonton, Alberta, 1988.
- [16] N. Nor-Azian and M. A. Adewumi, "Development of asphaltene phase equilibrium predictive model," SPE Eastern Regional Meeting, Pittsburgh, PA, USA, 1993.
- [17] R. Cimino, S. Correria, and P. A. Sacomani, "Thermodynamic modeling for prediction of asphaltene deposition in live-oils," *SPE International Symposium on Oilfield Chemistry*, San Antonio, TX, USA, 1995.
- [18] S. Kawanaka, S. J. Park, and G. A. Mansoori, "The role of asphaltene deposition in EOR gas flooding: A predictive technique," SPE /DOE Enhanced Oil Recovery Symposium, Tulsa, Oklahoma, 1988.
- [19] S. J. Park, "A thermodynamic polydisperse polymer model: Asphaltene flocculation, aggregation and deposition," PhD dissertation, University of Illinois, Chicago, USA, 1989.
- [20] R. Botet and J. Jullien, "Size distribution of clusters in irreversible kinetic aggregation," *Journal of Physics A: Mathematical and General*, vol. 17, pp. 2517-2530, 1984.
- [21] H. W. Yarranton, J. H. Masliyah, "Molar mass distribution and solubility modeling of asphaltenes," *AIChE Journal*, vol. 42, pp. 3533-3543, 1996.
- [22] E. Rogel, "Theoretical estimation of the solubility parameter distributions of asphaltenes, resins, and oils from materials," *Energy & Fuels*, vol. 11, pp. 920-925, 1997.
- [23] V. A. M. Branco, G. A. Mansoori, L. C. D. A. Xavier, S. J. Park, and H. Manafi, "Asphaltene flocculation and collapse from petroleum fluids," *Journal of Petroleum Science and Engineering*, vol. 32, pp. 217-230, 2001.
- [24] J. E. P. Monteagudo, P. L. C. Lage, and K. Rajagopal, "Towards a polydisperse molecular thermodynamic model for asphaltene precipitation in live-oil," *Fluid Phase Equilibria*, vol. 187, pp. 443-471, 2001.
- [25] L. X. Nghiem, D. A. Coombe, and S. M. F. Ali, "Compositional simulation of asphaltene deposition and plugging," SPE Annual Technical Conference and Exhibition, New Orleans, Louisiana, 1998.
- [26] A. A. Shinta, A. Firoozabadi, "Predicting phase behavior of water/reservoir-crude systems using the association concept," *SPE Reservoir Engineering*, vol. 12, pp. 131-137, 1997.
- [27] H. Toubia, G. A. Mansoori, "Equations of state for associating fluids (based on the analytic chain association theory)," *Fluid Phase Equilibria*, vol. 119, pp. 51-65, 1996.
- [28] M. Vafaie-Sefti, S. A. Mousavi-Dehghani, and M. Mohammad-Zadeh, "A simple model for asphaltene deposition in petroleum mixtures," *Fluid Phase Equilibria*, vol. 206, pp. 1-11, 2003.
- [29] K. J. Leontaritis and G. A. Mansoori, "Asphaltene flocculation during oil production and processing: A thermodynamic colloidal model," SPE International Symposium on Oilfield Chemistry, San Antonio, TX, USA, 1987.
- [30] A. Janardhan and G. A. Mansoori, "Fractal nature of asphaltene aggregation," *Journal of Petroleum Science and Engineering*, vol. 9, pp. 17-27, 1993.
- [31] A. I. Victorov and A. Firoozabadi, "Thermodynamic micellization model of asphaltene precipitation from petroleum fluids," *AIChE Journal*, vol. 42, pp. 1753-1764, 1996.
- [32] B. Dabir, M. Nematy, A. R. Mehrabi, H. Rassamdana, and M. Sahimi, "Asphalt flocculation and deposition - III. The molecular weight distribution," *Fuel*, vol. 75, pp. 1633-1645, 1996.
- [33] H. Rassamdana, M. Sahimi, "Asphalt flocculation and deposition: II. Formation and growth of fractal aggregates," *AIChE Journal*, vol. 42, pp. 3318-3332, 1996.
- [34] M. Sahimi, H. Rassamdana, and B. Dabir, "Asphalt formation and precipitation: Experimental studies and theoretical modeling," *SPE Journal*, vol. 2, pp. 157-169, 1997.

- [35] M. Sahimi and H. Rassamdana, "Formation, growth and precipitation of fractal molecular aggregates in porous media," *Physica A*, vol. 240, pp. 419-431, 1997.
- [36] J. A. Nelder and R. Mead, "A simplex method for function minimization," *Comput. J.* vol. 7, pp. 308-313, 1965.
- [37] A. R. Soleimany Nazar, B. Dabir, and M. R. Islam, "A multi-solid phase thermodynamic model for predicting wax precipitation in petroleum mixtures," *Energy Sources*, vol. 27, pp. 173-184, 2005.
- [38] R. A. Behrens and S. I. Sandler, "The use of semicontinuous description to model the C_7^+ fraction in equation of state calculations," *SPE Reservoir Engineering*, vol. 3, pp. 1041-1047, 1988.
- [39] M. R. Riazi, T. E. Daubert, "Prediction of molecular-type analysis of petroleum fractions and coal liquids," *Ind. Eng. Chem. Process Des. Dev.* vol. 25, pp. 1009-1015, 1986.
- [40] D. L. Katz and A. Firoozabadi, "Predicting phase behavior of condensate / crude oil systems using methane interaction coefficients," *Journal of Petroleum Technology*, vol. 30, pp. 1649-1655, 1978.
- [41] M. R. Riazi, T. E. Daubert, "Simplify property predictions," *Hydrocarbon Processing*, vol. 59, pp. 115-116, 1980.
- [42] M. R. Riazi, T. E. Daubert, "Characterization parameters for petroleum fractions," *Ind. Eng. Chem. Res.* vol. 26, pp. 755-759, 1987.
- [43] M. R. Riazi, T. A. Al-Sahhaf, "Physical properties of heavy petroleum fractions and crude oils," *Fluid Phase Equilibria*, vol. 117, pp. 217-224, 1996.
- [44] H. Pan and A. Firoozabadi, "Pressure and composition effect on wax precipitation: Experimental data and model results," *SPE Production & Facilities*, vol. 12, pp. 250-258, 1996.
- [45] M. G. Broadhurst, "An analysis of the solid phase behavior of the normal paraffins," *Journal of Research of the National Bureau of Standards - A. Physics and Chemistry*, vol. 66A, pp. 241-249, 1962.
- [46] K. S. Pedersen, P. Skovborg, and H. P. Ronningsen, "Wax precipitation from North Sea crude oils. 4. Thermodynamic modeling," *Energy & Fuels*, vol. 5, pp. 924-932, 1991.
- [47] M. R. Riazi, T. A. Al-Sahhaf, "Physical properties of n-alkanes and n-alkylhydrocarbons: Application to petroleum mixtures," *Ind. Eng. Chem. Res.*, vol. 34, pp. 4145-4148, 1995.
- [48] C. H. Twu, "An internally consistent correlation for predicting the critical properties and molecular weights of petroleum and coal-tar liquids," *Fluid Phase Equilibria*, vol. 16, pp. 137-150, 1984.
- [49] N. E. Burke, R. E. Hobbs, and S. F. Kassou, "Measurement and modeling of asphaltene precipitation," *JPT*, vol. 42, pp. 1440-1446, 1990.
- [50] R. K. Srivastava and S. S. Huang, "Asphaltene deposition during CO₂ flooding: A laboratory assessment," SPE 37468, SPE Production Operations Symposium, Oklahoma, 1997.
- [51] H. Pan and A. Firoozabadi, "Thermodynamic micellization model for asphaltene precipitation from reservoir crude at high pressures and temperatures," SPE 38857, SPE Annual Technical Conference and Exhibiton, San Antonio, Texas, USA, 1997.
- [52] L. X. Nghiem and D. A. Coombe, "Modeling Asphaltene Precipitation during primary depletion," *SPE Journal*, vol. 2, pp. 170-176, 1997.
- [53] Z. Yang, C. F. Ma, X. S. Lin, J. T. Yang, and T. M. Guo, "Experimental and modeling studies on the asphaltene precipitation in degassed and gas-injected reservoir oils," *Fluid Phase Equilibria*, vol. 157, pp. 143-158, 1999.